


Article

Evaluation of Groundwater Sources, Flow Paths, and Residence Time of the Gran Desierto Pozos, Sonora, Mexico

Hector A. Zamora ^{1,*}, Benjamin T. Wilder ², Christopher J. Eastoe ^{1,†}, Jennifer C. McIntosh ³, Jeffrey Welker ⁴  and Karl W. Flessa ¹

¹ Department of Geosciences, University of Arizona, Tucson, AZ 85721, USA

² Desert Laboratory on Tumamoc Hill, University of Arizona, Tucson, AZ 85719, USA

³ Department of Hydrology and Atmospheric Sciences, University of Arizona, Tucson, AZ 85721, USA

⁴ Department of Biological Sciences, University of Alaska Anchorage, Anchorage, AK 99508, USA

* Correspondence: hzamora@email.arizona.edu

† Retired.

Received: 5 August 2019; Accepted: 28 August 2019; Published: 30 August 2019



Abstract: Environmental isotopes and water chemistry distinguish water types, aquifer recharge mechanisms, and flow paths in the Gran Desierto and Colorado River delta aquifer. The aquifer beneath the Gran Desierto supports a series of spring-fed wetlands, locally known as pozos, which have provided vital water resources to diverse flora and fauna and to travelers who visited the area for millennia. Stable isotope data shows that local recharge originates as winter precipitation, but is not the main source of water in the pozos. Instead, Colorado River water with substantial evaporation is the main component of water in the aquifer that feeds the pozos. Before infiltration, Colorado River water was partially evaporated in an arid wetland environment. Groundwater followed flow paths, created by the Altar Fault, into the current location of the pozos at Bahía Adair. Mixing with seawater is observed at the pozos located near the coast of the Gulf of California. The wetlands or other natural settings that allowed recharge to the aquifer feeding the pozos no longer exist. This leaves the pozos vulnerable to major groundwater pumping and development in the area.

Keywords: groundwater; environmental isotopes; Colorado River delta

1. Introduction

Observations and studies in the early twentieth century along the Colorado River and its delta documented wetland and riparian ecosystems swarming with life, sustained by the muddy waters of the then mighty Colorado [1,2]. Today, water-management practices, including dams and the over-allocation of Colorado River water, have drastically reduced these once vast ecosystems. The river no longer reaches the lower part of the delta, but a string of coastal wetlands that harbor oases of plant and animal communities, and an underground aquifer of unknown extent still exist in the area [3,4].

Adjacent to the upper Gulf of California and the Colorado River Delta is the most extensive sand dune field of North America, the Gran Desierto de Altar (Figure 1). A series of wetlands and freshwater springs, or pozos as they are locally known, are found on the westward coastal fringe of the massive dune field (Figure 2). These oases represent one of the most critical biological and cultural resources in this dry borderland region of the Sonoran Desert [5,6]. The spring-fed water bodies support a diversity of flora that contrasts with the surrounding desert, due to the water's availability and relatively low salinity [7]. The pozos support at least 26 species of vascular plants [3], and a variety of terrestrial and avian fauna congregates around them.



Figure 1. Location of the Colorado River delta, Altar Basin, and major geographical and geological features. Organ Pipe Cactus National Monument (OPCNM, discussed below) is located ~100 km northeast from the study area and is shown as a red triangle in the upper map. The dashed red line in the bottom map separates the floodplain (west) from the Yuma and San Luis mesas (east). The dashed blue line labeled the Gila River represents a dry river bed. Blue stars in the bottom map show the general location of the pozos.



Figure 2. The pozos of El Gran Desierto. (A) Pond in La Salina, (B) pozo Tres Ojitos, (C) cottonwood (*Populus fremontii*) near La Salina, and (D) prehistoric shell midden at La Salina. Photo credits: Benjamin T. Wilder and Benjamin M. Johnson.

The remote freshwater springs were also destinations of multi-day pilgrimages along the historic Salt Trails where indigenous inhabitants navigated through the dune field to the sea to collect salt [8,9]. Oxygen isotope ratios in shells from prehistoric middens (Figure 2D) and carbon-14 (^{14}C) ages from buried charcoal suggest that people visited the northern Sonoran coast during the fall and winter to harvest fish and shellfish soon after the stabilization of the early Holocene sea level rise around 7000 yrs. B.P. [10], if not before [11,12]. Pioneering explorers seeking an overland route to California also used the pozos as a watering stop. Observations relative to early explorers' descriptions and photos from the early nineteenth centuries suggest that the pozos have not changed drastically during recent centuries [8].

Previous studies in the area have attempted to decipher the source of recharge of the pozos [3]. Nonetheless, the underpinning questions of age and origin of the pozos water have remained unsolved. In this study, we use environmental tracers to advance our understanding on these enigmatic oases. Our initial hypotheses were that (1) the systematic study of oxygen and hydrogen isotopes would refine the understanding of groundwater sources in the Gran Desierto aquifer and the pozos; (2) the radioactive isotopes tritium (^3H) and ^{14}C would provide an estimate of groundwater residence times; and (3) the combination of these environmental isotopes, major ion chemistry, and the features of the local hydrology would provide information to evaluate groundwater dynamics (e.g., flow paths) throughout this transboundary aquifer. This information is relevant because of anticipated severe droughts and water shortages in the region [13,14], and is an important contribution needed to manage the hydrological, biological, and cultural resources of the Gran Desierto wetlands.

2. Materials and Methods

2.1. Study Area

The Gran Desierto is a Late Pleistocene dune field that extends from the eastern end of the Colorado River delta to the Sierra El Pinacate (El Pinacate) in Sonora [15,16]. It is one of the driest and hottest deserts in North America where maximum temperatures reach 46 °C, and the mean annual temperature is 23 °C [17]. Precipitation occurs as sporadic, cyclonic events during winter, and rare localized convective events during summer with an annual average between 53 mm and 57 mm [17].

The study area is bounded to the northeast by northwest-southeast mountain ranges consisting of igneous and metamorphic rocks of the Cretaceous age (Gila Range, Tinajas Altas, and Sierra El Rosario), and to the east by basaltic flows of the Pleistocene to late Holocene age (Sierra El Pinacate). The Altar Basin covers the area between San Luis Rio Colorado and Bahia Adair (Figure 1). This area was once part of the delta complex, but now is an inactive, subsidiary basin above the level subject to flooding by the Colorado River [18].

The Cerro Prieto fault, part of the San Andreas Fault system, traverses the study area and continues into the Gulf of California [19] (Figure 1). Strike-slip movement along the Cerro Prieto fault system is estimated to be as much as 60 mm/year [20,21]. The eastern side of the Altar Basin is limited by the seismically inactive Altar Fault [18] (Figure 1). Both faults are northwest trending, dip to the west, have significant dextral offset, and drop the southwestern side down.

The principal aquifer beneath the Colorado River valley and the mesas (fluvial terraces) of Yuma and San Luis occurs within a series of gravels [22], and groundwater generally moves in a northeast to southwest direction (Figure 3). This alluvial aquifer becomes confined towards the coast as a result of the presence clay layers with hydraulic conductivity of 0.001 cm/hr, and artesian pressure develops [3]. Thick and extensive coastal salt flats (sabkhas) barren of vegetation, and believed to be of paleo-deltaic origin [23], cover several areas along the coast particularly northwest of Bahía Adair. Along these coastal salt flats, pozos develop in locations where the permeability of the clay increases because of desiccation cracking, flocculation due to ion exchange, or digging by local fauna in the search of freshwater [3]. These processes expose a sandy layer containing groundwater with a vertical head gradient of ~0.40 m/m, and a hydraulic conductivity 243 cm/hr [3].

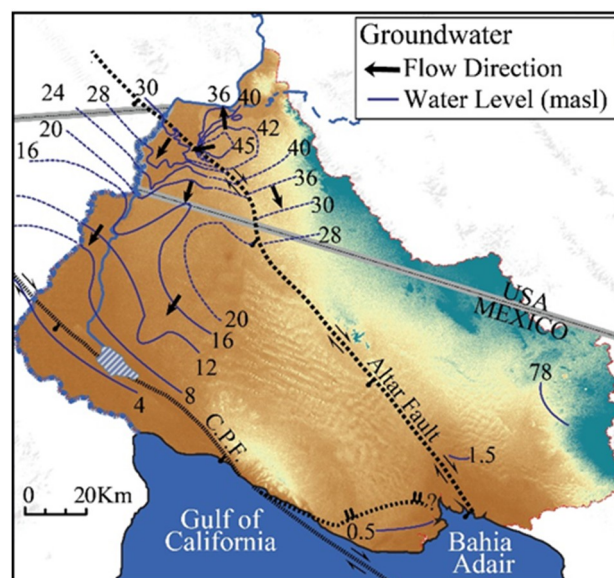


Figure 3. Groundwater levels in 2010. Contours represent water table elevation in meters above sea level (based on data from [24–26]).

2.2. Data Collection and Analysis

In order to further investigate the origin and dynamics of the groundwater system feeding the pozos, we collected surface and groundwater samples on several trips to the area between 2013 and 2017, and during different times of the year (Figure 4). Thirty-four surface water samples were collected from the pozos and ten from the Ciénega de Santa Clara (Ciénega), a wetland supported by brackish agricultural return flow derived from the Wellton-Mohawk Irrigation Drainage District of Arizona (see Figure 1 for location of the Ciénega). The Wellton and Mohawk valleys are irrigated with Colorado River water. The wetland was sampled because it represents the composition of evaporated Colorado River water and can be compared with the pozos.

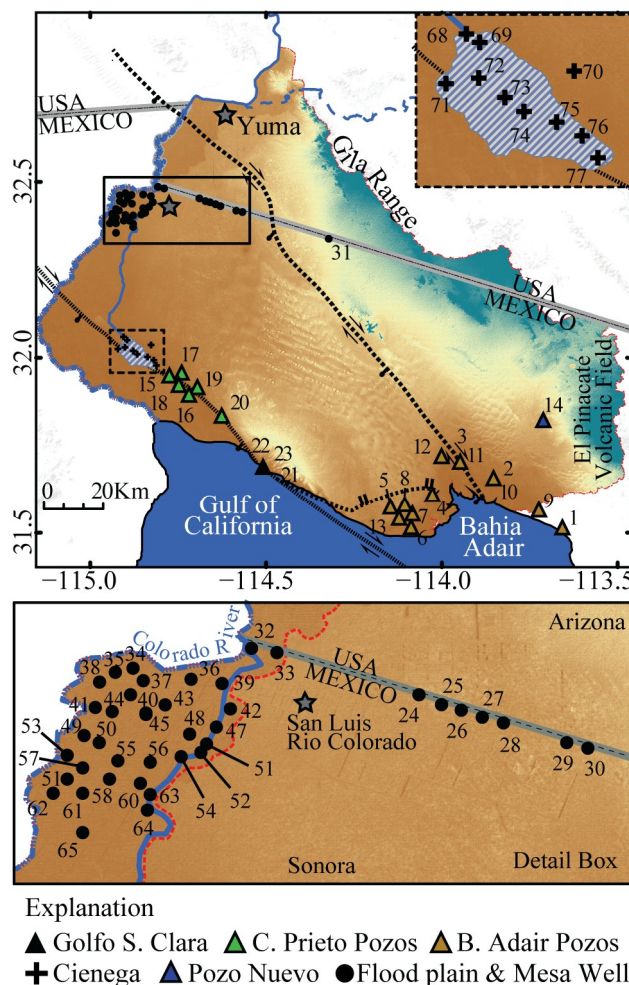


Figure 4. Location of sampling sites in study area. Red dashed line in detail box separates floodplain (west) from the San Luis and Yuma mesas (east).

The pozos were drained using a hand bucket and allowed to refill to obtain a sample not affected by evaporation (where this was possible). Groundwater samples were collected from two wells available in the pozos’ vicinity. Two water samples were obtained from auger holes adjacent to the pozos in order to minimize evaporation. These holes were hand-drilled in the clay layer beneath the surface. The pozos samples were divided into two sub-groups. Those located along the Altar Fault in the vicinity of Bahía Adair were designated as Bahía Adair (Adair) pozos, and those located along the escarpment dividing the delta from the San Luis Mesa were designated as Cerro Prieto Fault (Cerro Prieto) pozos. Water samples collected from auger holes and wells are included with the Adair pozos, but are differentiated in Table S1. Sampling site 14 (locally known as Pozo Nuevo), is at the base of the west side of El Pinacate at an elevation of 78 m a.s.l., and is separated from both

groups (see Figure 4). This private well was purged for five well volumes to obtain a representative, non-evaporated groundwater sample. Rainfall samples were collected using rain gauges scattered throughout the region. A thin layer of mineral oil was added to the rain-collecting devices to prevent evaporation. The accumulated rainfall was recovered from all stations during field visits in late October and late March during two years (2015 and 2016). Three tap water samples (sites 21–23 in Figure 4) were obtained from El Golfo de Santa Clara's supply because wells were unavailable for sampling.

Temperature, pH, and electrical conductivity were measured in the field after each parameter had stabilized using a YSI 556 Multiparameter System sonde calibrated with a standard pH buffer (4, 7, and 10) and conductivity (1413 μS) solutions. Samples collected for stable isotopes analysis (O, H, and C) were filtered through a 0.45- μm nylon filter and kept in 20 mL glass vials with no headspace. Unfiltered water samples were collected for age tracers (^3H and ^{14}C) using rinsed 1-L HDPE and amber borosilicate glass bottles, respectively. Samples for ions and alkalinity were filtered with 0.45- μm nylon filters into 30 mL HDPE bottles. Cation samples were preserved by adding two drops of concentrated optima grade HNO_3 . All samples were kept on ice during field collection and then refrigerated at 4 $^\circ\text{C}$.

Values for $\delta^{18}\text{O}$ and $\delta^2\text{H}$ were determined in the Environmental Isotope Laboratory, Department of Geosciences, University of Arizona, using a Finnigan Delta-S mass spectrometer with automated CO_2 equilibration and Cr reduction attachments. The $\delta^{18}\text{O}$ and $\delta^2\text{H}$ values are reported in delta notation where:

$$\delta = (R/R_{\text{std}} - 1) \times 1000 (\text{‰}). \quad (1)$$

R is the ratio of the heavier over the lighter isotope in the sample, and R_{std} is the isotope ratio of Vienna standard mean ocean water (VSMOW). Calibration followed the method of Coplen [27], using international standards VSMOW and standard light Antarctic precipitation (SLAP). The analytical precisions (1σ) for these techniques were 0.9‰ for $\delta^2\text{H}$ and 0.08‰ for $\delta^{18}\text{O}$.

Values for $\delta^{13}\text{C}_{\text{DIC}}$ were measured on a Thermo-Finnigan Delta Plus XL continuous-flow gas-ratio mass spectrometer coupled with a Gasbench automated sampler. Samples were reacted for more than 1 h with phosphoric acid at room temperature in Exetainer vials flushed with He gas. Standardization is based on NBS-19 and NBS-18 and precision was + 0.30‰ or better (1σ). Values for $\delta^{13}\text{C}$ are expressed in delta notation relative to the Vienna Pee Dee Belemnite (VPDB) standard.

Tritium values were measured by liquid scintillation counting on electrolytically enriched water in a Quantulus 1220 Spectrophotometer. The detection limit was 0.5 TU for nine-fold enrichment and 1500 min of counting. One tritium unit (TU) is equivalent to one tritium atom in 1018 atoms of hydrogen. Carbon-14 was measured as liberated CO_2 reduced to graphite at the NSF-Arizona AMS facility. Carbon-14 results are reported as percent modern carbon (pMC) relative to NBS standards Oxalic Acid I and II. Anion concentrations (excluding HCO_3^- and CO_3^{2-}) were determined using a Dionex Ion Chromatograph model 3000 with an AS23 analytical column (precision + 2%) at the University of Arizona Department of Hydrology and Water Resources. Alkalinity was determined by the Gran-Alkalinity titration method [28] within 24 h of collection. The HCO_3^- and CO_3^{2-} concentrations were determined using the PHREEQC speciation model [29]. The analyses for cations were performed using an Elan DRC-II Inductively Coupled Plasma–Mass Spectrometer at the University of Arizona Laboratory for Emerging Contaminants (ALEC).

New (this study) and available isotope and solute chemistry data [3,30–32] for groundwater and surface water samples in the Colorado River delta and the Altar Basin are compiled and presented in Table S1. Rainfall data collected as part of this study are insufficient to calculate long-term mean $\delta^{18}\text{O}$ and $\delta^2\text{H}$ values. For this reason, rainfall stable isotope data were obtained from the United States Network for Isotopes (USNIP) station located at the Organ Pipe Cactus National Monument (OPCNM) [33]. These data are a collection of individual events registered between 1990 and 2006 (Table S2). OPCNM is located at an elevation of 515 m above sea level and ~100 km northeast from the study. OPCNM's elevation is similar to the average elevations seen at El Pinacate where aquifer recharge is likely to occur.

Additionally, major ion chemistry for rainfall was obtained from the National Atmospheric Deposition Program (NADP) station also located at OPCNM [34]. These data represent individual events collected between 1980 and 2017. Bicarbonate is not reported in the NADP samples. In these cases, HCO_3^- was estimated by balancing the charge among the major ions, assuming it to be the missing anion. Then, these samples were plotted on a Piper Diagram for hydrochemical characterization (Figure 5).

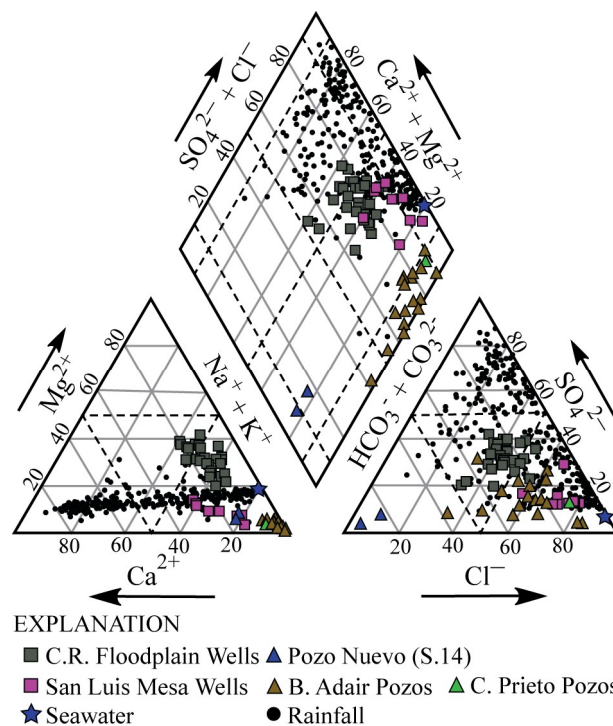


Figure 5. Piper diagram showing data for rainfall samples collected at the Organ Pipe Cactus National Monument (OPCNM), Colorado River (C.R.) floodplain well samples, San Luis Mesa well samples, and pozos water samples. Bicarbonate was used to balance the charge among major ions where it was not reported.

3. Results

3.1. Rainfall

There is a wide distribution of solutes, but in general, rainfall is dominated by the Ca– SO_4 and Na–Cl facies. Only a few samples plot within the Ca– HCO_3 facies. Stable isotope data for winter precipitation (November to April) followed a trend with a slope of 7.9 and a y-intercept of 9.89 ($R^2 = 0.91$, Figure 6A); almost identical to the global meteoric water line (GMWL) [35]. Data for summer precipitation (May to October) followed a trend with a slope of 6.43 and a y-intercept of -2.11 ($R^2 = 0.89$, Figure 6A). The weighted mean ($\delta^{18}\text{O}$, $\delta^2\text{H}$) values were -5.7‰ and -38‰ for yearly rainfall, -7.2‰ and -47‰ for winter rainfall, and -4.3‰ and -29‰ for summer precipitation (Figure 6B).

3.2. Ciénega de Santa Clara

Surface water samples from the Ciénega had Cl^- concentrations between 550 mg/L and 54,492 mg/L, and SO_4 concentrations between 251 mg/L and 9,653 mg/L. The concentrations of these solutes increased southward towards the Gulf of California (Table S1). The $\delta^{18}\text{O}$ values ranged between -10.6‰ and $+6.0\text{‰}$, and the $\delta^2\text{H}$ values ranged between -88‰ and $+8\text{‰}$ (Figure 7A). The highest ($\delta^{18}\text{O}$, $\delta^2\text{H}$) values were also located in the southern part of the Ciénega near the tidal flats (sites 76 and 77). Most of the water samples fell to the right of the GMWL. The regression line ($\delta^{18}\text{O}$ and $\delta^2\text{H}$) had a slope of 5.8 (Figure 7A). The slope was within the range observed by other studies in the area (slopes between

5 and 6; [36]) and was characteristic of evaporated Colorado River water [37,38]. This evaporation line is shown in Figure 7 as the Colorado River evaporation trend (CRET).

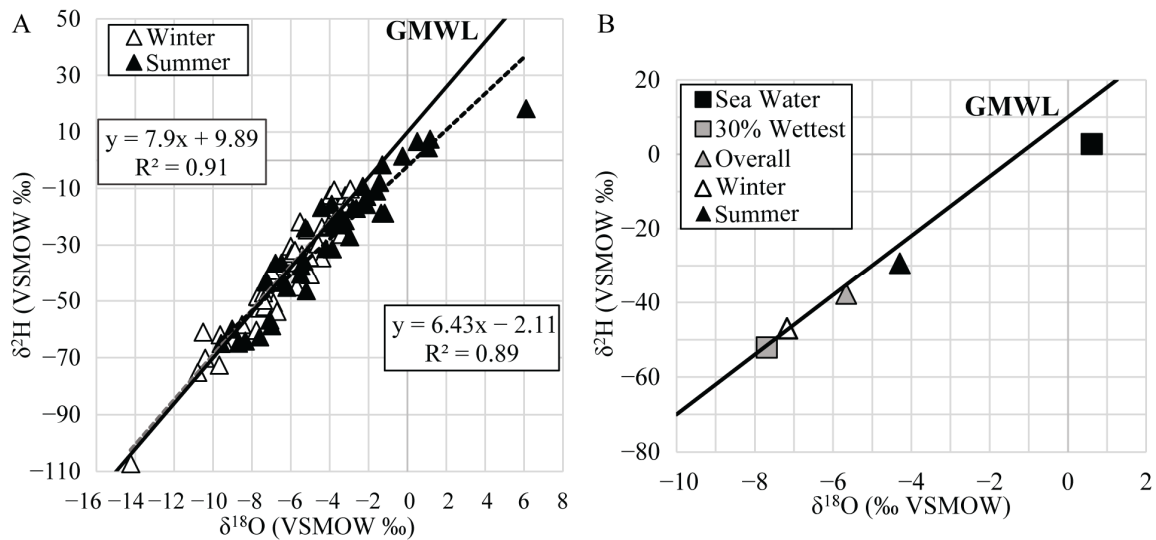


Figure 6. (A) $\delta^2\text{H}$ vs. $\delta^{18}\text{O}$ values for individual precipitation events collected at OPCNM. (B) Amount-weighted average $\delta^{18}\text{O}$ and $\delta^2\text{H}$ values for overall, winter, summer precipitation, and 30% wettest events for samples in 5A.

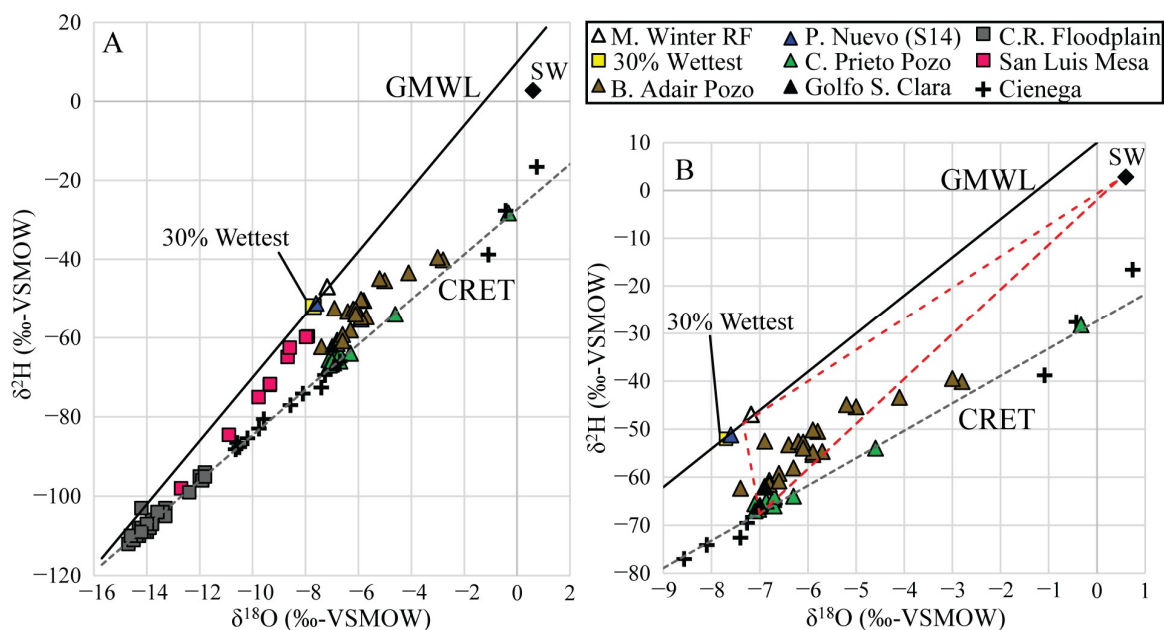


Figure 7. (A) $\delta^2\text{H}$ vs. $\delta^{18}\text{O}$ values for surface and groundwater from Colorado River floodplain, San Luis Mesa, Cienega, mean winter rainfall (RF), 30% wettest rainfall events at OPCNM rain gauge, and the pozos relative to the global meteoric water line (GMWL), and Colorado River evaporation trend (CRET). (B) Detailed view showing the pozos samples relative to the GMWL and CRET. Red dashed triangle shows the mixing trend that would be followed by mixing evaporated Colorado River water ($\delta^{18}\text{O} = -6.8\text{‰}$, $\delta^2\text{H} = -67\text{‰}$), local recharge, and seawater (SW).

3.3. Colorado River Floodplain and San Luis Mesa

Colorado River floodplain samples are divided between Ca-SO₄ and Na-Cl facies (Figure 5). Groundwaters in the eastern side of the San Luis Mesa show Na⁺ and Cl⁻ as the predominant ions, and evolve into a Ca-SO₄ facies as they move westward and mix with Colorado River water.

These groundwaters are undersaturated with respect to halite, gypsum, and anhydrite allowing Na^+ , Cl^- , Ca^{2+} , and SO_4^{2-} concentrations to increase along the flow paths. The $\delta^{18}\text{O}$ values for Colorado River floodplain groundwaters range between -11.8‰ and -14.7‰ , and $\delta^2\text{H}$ values range between -94‰ and -112‰ . The $(\delta^{18}\text{O}, \delta^2\text{H})$ values for the San Luis Mesa groundwaters range between -7.9‰ and -12.7‰ , and between -60‰ and -98‰ , respectively (Figure 7).

3.4. Gran Desierto Pozos and El Golfo Groundwater

The waters of the pozos were characterized as Na–Cl facies, with the exception of sites 9 and 14, which had a Na– HCO_3 chemistry (Figure 5). Site 14 (Pozo Nuevo), at the base of El Pinacate and away from any major stream, had $(\delta^{18}\text{O}, \delta^2\text{H})$ values of -7.6‰ and -51‰ . The $(\delta^{18}\text{O}, \delta^2\text{H})$ values for the Adair pozos ranged between -3‰ and -8‰ , and between -40‰ and -62‰ , respectively (Figure 7). The $(\delta^{18}\text{O}, \delta^2\text{H})$ values for the Cerro Prieto pozos and the El Golfo samples showed less variability, excluding sample 19 (highly evaporated), and ranged between -6.3‰ and -7.1‰ , and -62‰ and -67‰ (Figure 7), respectively.

Tritium activities were below detection levels for all pozos samples at both the Adair and Cerro Prieto locations (Figure 8A). Carbon-14 values varied between 10 and 90 pMC in the Adair pozos, including site 14 at Pozo Nuevo, which had a value of 87 pMC (Figure 8B). The ^{14}C values in the Cerro Prieto pozos ranged between 3 and 25 decreasing from north to south. There was no clear correlation between ^{14}C (or ^3H) and $\delta^{18}\text{O}$ values.

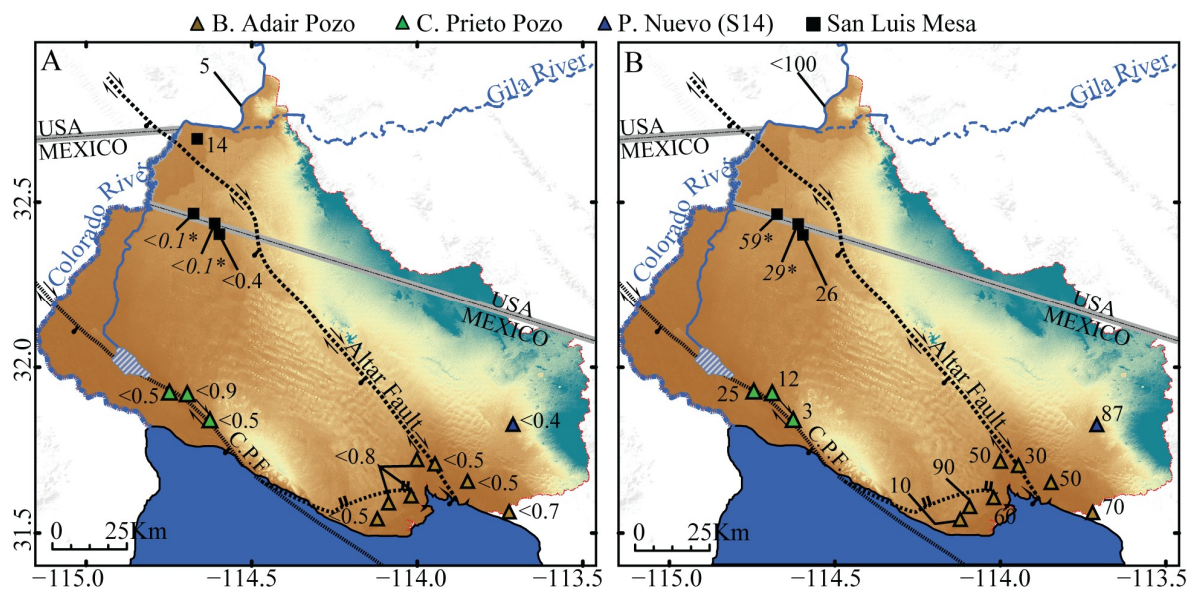


Figure 8. (A) Tritium (TU) data for water samples in the study area. (B) Carbon-14 (pMC) for water samples in the study area. Data shown with asterisk (*) from [24].

4. Discussion

4.1. Rainfall and Local Recharge

The chemistry of regional rainfall is variable and is not restricted to a particular hydrochemical composition. However, the Na–Cl and Ca– SO_4 compositions predominated (Figure 5). The cation portion of the Piper diagram showed a linear trend of rainfall samples plotting between Ca^{2+} and Na^+ . One possible explanation of this pattern could be related to the source of the water vapor for precipitation. Rainfall formed from vapor originating near the Pacific coast will have similar ion ratios to those of sea water, through release and dissolution of marine aerosols [39], and will plot in the Na–Cl portion of the Piper diagram. Rainfall moving inland from more distant sources (e.g., Gulf of Mexico, East Pacific) into the area might have higher concentrations of Ca^{2+} and SO_4^{2-} , relative to Na^+

and Cl^- , as marine-derived solutes fallout near the coast and continental dust containing gypsum is rapidly acquired and dissolved [39].

The ($\delta^{18}\text{O}$, $\delta^2\text{H}$) values observed at site 14 (Pozo Nuevo) plot near the GMWL and represent locally recharged groundwaters (-7.6‰ and -51‰). Similar groundwater values have been observed in other catchments located in the lower Gila basin and the Sonoyta River basin in southwestern Arizona, and adjacent to the study area [40,41]. The local recharge value was slightly lower than the weighted average ($\delta^{18}\text{O}$, $\delta^2\text{H}$) values for winter rainfall at the OPCNM rain gauge (-7.2‰ and -47‰ , Figure 7).

Long-term records of ($\delta^{18}\text{O}$, $\delta^2\text{H}$) values in precipitation and groundwater in tropical and sub-tropical areas show that groundwater recharge was biased to heavy monthly rainfall exceeding the ~70th intensity percentile (or the 30% most intense events; [42]). In the Sonoran Desert, the amounts and stable isotope data of rainfall show that events with totals above the 60th percentile usually had lower ($\delta^{18}\text{O}$, $\delta^2\text{H}$) values than the weighted winter averages (e.g., Figure 9). In fact, the amount-weighted average $\delta^{18}\text{O}$ and $\delta^2\text{H}$ values for the largest 30% of the rainfall events (-7.5‰ , and -50‰) were almost identical to locally recharged groundwaters (-7.6‰ and -51‰ , site 14).

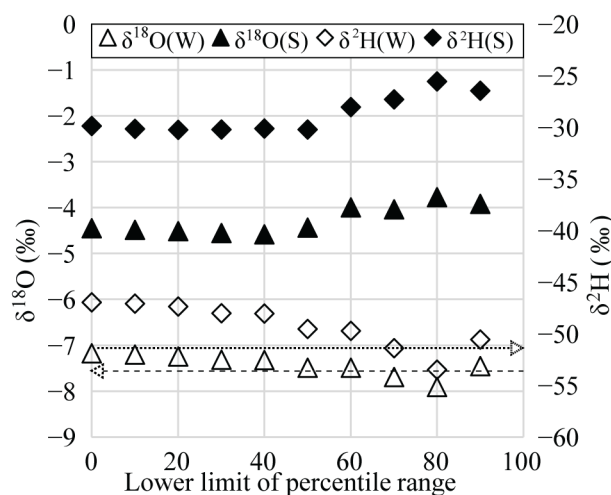


Figure 9. Amount-weighted average $\delta^{18}\text{O}$ and $\delta^2\text{H}$ values as a function of the size of rain events. As an example, the points for 80% correspond to an amount-weighted average of the largest 20% of rain events. Dashed (dotted) line points to $\delta^{18}\text{O}$ ($\delta^2\text{H}$) value of local recharge in the region (site 14). Plot based on Table S2 for precipitation at OPCNM. S = summer, W = winter.

Based on these observations, it is reasonable to conclude that recharge at the base of El Pinacate is limited to the largest 30% of the rainfall events. During these events, which occur during winter, the amount of water was large enough and the environmental conditions were optimal for infiltration and percolation of moisture into the water table. This pattern has been observed in other regions of southwest Arizona [36].

4.2. Origin of the Gran Desierto Pozos

Water samples collected from the pozos and nearby wells along the coast had different ($\delta^{18}\text{O}$, $\delta^2\text{H}$) values relative to groundwaters in the lower Colorado River floodplain and in the San Luis Mesa (Figure 7A). Previous studies [3] hypothesized that water in the pozos was derived as local recharge flowing from El Pinacate towards the coast (Figure 1). While site 14 was consistent with the local recharge as discussed in the previous section, the pozos (both Adair and Cerro Prieto), well, and tap water samples from El Golfo plotted far from the GMWL, and require further explanation (Figure 7A,B).

Most of the Cerro Prieto pozos plotted in a cluster with $\delta^{18}\text{O}$ values between -6.3‰ and -7.1‰ along the CRET. The association of the pozos samples with the CRET suggests that they consist of evaporated Colorado River water. The plotting position of this cluster approaches Colorado River water that has undergone ~40% evaporation at 60% relative humidity according to calculations made

by H.A.Z. [43] using the method described by Clark and Fritz [44]. Some of the Adair pozos samples plot near the Cerro Prieto pozos cluster, but there was significantly more scatter among the Adair pozos, and they also seem to follow a different trend away from the CRET (dashed polygon in Figure 7B). The water table elevation of the Adair pozos was no higher than 1.5 m a.s.l., and these seem to be located near the fresh groundwater and seawater interface. There is a possibility that some seawater intrudes into the fresh groundwater system. Higher-than-average tides during spring tides and tidal surges caused by hurricanes (rare, but occur in the study area) would certainly force seawater inland. Seawater intrusion would cause some of the east Adair pozos samples to plot in a field between evaporated Colorado River water and seawater as shown in Figure 7B.

The monovalent ions Cl^- and Br^- provide a useful tracer combination to identify salinity sources in groundwater. Bromide is rejected during the process of halite precipitation, and the Cl/Br mass ratio of solid NaCl is usually 2–3 orders of magnitude higher than in the original waters (~ 5000) [45]. Available data from the Colorado River water near Yuma, Arizona (USGS Stations 09429600 and 09521100; [30]) were consistent with a trend line resulting from the dissolution of halite (Figure 10A,B). Water samples from the pozos plotted close to a seawater dilution or mixing trend (Figure 10A,C). There are two alternatives that explain this observation. Given the location of the pozos near the coast, it is likely that there is a percentage of seawater in the pozos. This is consistent with the pozos-seawater trend observed in the stable isotope data and supports field observations [23] that hypothesized the intrusion of seawater into the pozos closest to the coast. The percentage of seawater in the solution would depend on location, but mass balance calculations using $\delta^{18}\text{O}$ suggest that it would not exceed 25%.

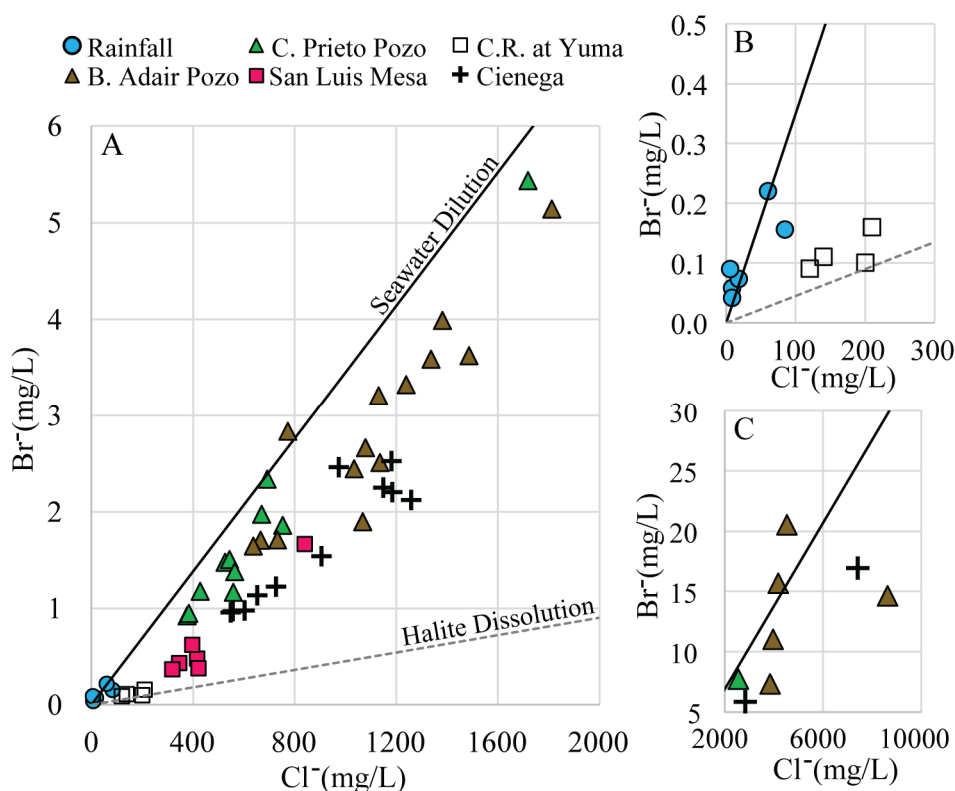


Figure 10. (A) Br^- vs. Cl^- (mg/L) values for water samples in the study area. (B) Detailed view of the lower end of graph A. (C) Extension of graph A to higher salinity. Colorado River water (C.R.) at Yuma obtained was from USGS Station 09404200 [30].

The other possibility is the dissolution of marine-derived aerosols. The Cl/Br mass ratio in local precipitation ranges between 150 and 274. These values are similar, but lower than the marine Cl/Br mass ratio of 290 [46], and are likely due to the presence of organobromine compounds including CH_3Br

and $C_2H_4Br_2$. These compounds could have been originated as agricultural pesticides in the extensive Mexicali or San Luis valleys or as natural metabolites in marine organisms [47]. Constant dissolution of marine-derived aerosols would cause samples to plot along the seawater dilution trend. However, this mechanism by itself would not explain the observed mixing trend between evaporated Colorado River water and seawater observed in Figure 7B. Freshwater–seawater mixing and dissolution of marine aerosols not only affect Cl^- and Br^- , but also SO_4^{2-} concentrations. Figure 11 shows Cl^-/SO_4^{2-} ratios of waters in the study area seem to have a tendency to plot towards the seawater ratio likely also as a direct result of freshwater–seawater mixing and dissolution of marine aerosols.

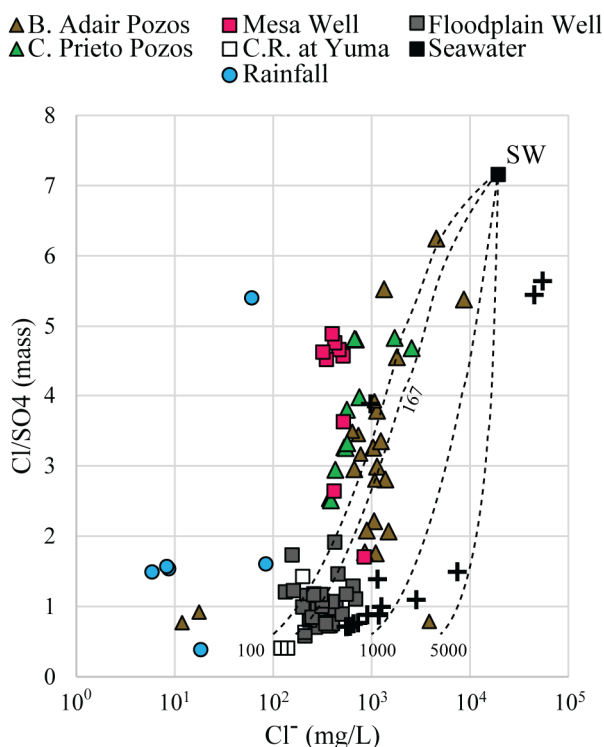


Figure 11. Cl^-/SO_4^{2-} (mass) vs. Cl^- concentration (mg/L, log scale) for surface and groundwaters in this study. Dashed lines show hypothetical mixing lines between seawater (SW)—or whole salt as aerosols—and Colorado River water.

A single mixing relationship between Colorado River water and seawater (in terms of Cl^- and Br^-) does not explain the variability observed in the pozos samples. Figure 12 shows different mixing lines for seawater with diverse river water compositions. The chemical compositions of the pozos samples are likely the result of mixing between Colorado River water with variable starting chemical compositions, and seawater. The variability in the starting composition of Colorado River water, in terms of Cl^- , could be explained in part by changes in the amount of salt input from evaporites, and evaporation. As previously discussed, water in the pozos seems to have undergone up to 40% evaporation from its original Colorado River composition, affecting the original Cl^- concentration.

4.3. Conceptual Model

Recharge to the pozos was subjected to an evaporative process at the surface prior to infiltration and percolation into the water table (Figure 13). Evaporation causes the pozos samples to plot along the CRET. This process is assumed to occur prior to infiltration, because groundwater samples collected from wells (sites 9 and 12), and tap water samples (municipal supply; sites 21, 22, 23) plot along the CRET and care was taken during collection to prevent evaporation. In modern times, ($\delta^{18}O$, δ^2H) values similar to the pozos (-6.8 and -67 ; Figure 7B) are only found along the Colorado River in highly evaporative environments such as the Ciénega, and Topock Marsh [38]. Clay layers across

the floodplain and the San Luis and Yuma Mesa deposited in a low-energy environment could be vestigial surfaces showing the possible location of such settings [22,24]. These environments are no longer found along the highly engineered floodplain of the Colorado River.

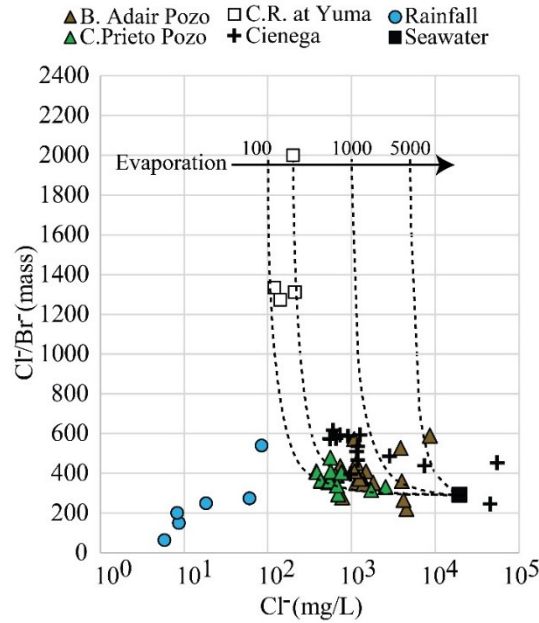


Figure 12. Cl^-/Br^- (mass) vs. $\log Cl^-$ (mg/L) for surface and groundwaters used in this study. Dashed lines show hypothetical mixing lines between seawater—or whole salt as aerosols—in one end, and Colorado River water with different Cl^- concentrations at the other.

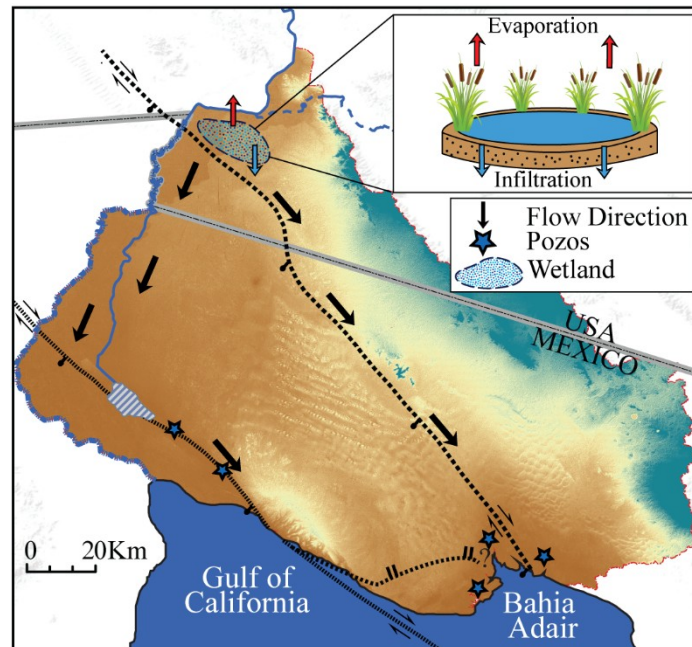


Figure 13. Schematic diagram showing recharge mechanisms. Recharge to the pozos was subjected to an evaporative process in a wetland environment prior to infiltration. Groundwater then followed a preferential flow path along the major faults in the area.

After infiltration and percolation, the direction of groundwater flow was influenced by the major faults in the study area. Faults are known to affect flow patterns in aquifers [48]. The pozos are conspicuously located along or near the Cerro Prieto and the Altar faults. It seems that groundwater

flow and discharge was focused along the faults. The Ciénega is also situated along the Cerro Prieto Fault, in an abandoned meander within the historical alluvial plain of the Colorado River. The presence of low permeability material, such as fault gouge, mineralization, and clay smearing might hamper flow across the fault, and develop a strongly anisotropic permeability near the Altar Fault zone [24]. The combination of a strong hydraulic gradient generated in the former recharge zones near Yuma, where a wetland environment could have been located in the past, and the fault-related permeability allowed groundwater to flow for tens of kilometers likely following old alluvial channels now buried under the dunes of the Gran Desierto [3] (Figure 4).

Age tracers suggest that none of the recharge for groundwater discharging at present in the pozos occurred in the last ~65 years. Tritium activities are below detection levels in all the pozos samples (Figure 8A). This is different from modern Colorado River water near Yuma, which has a value of ~5 TU and even higher values in the past decades as a result of nuclear testing [49]. Carbon-14 values were also lower in the pozos water samples than in Colorado River water at Yuma (> 100 pMC, Figure 8B). Corrected ^{14}C ages were calculated for sites 13 and 20 using the Fontes–Garnier model [50]. For these two sites, water is constantly running, the point of discharge is free of any vegetation that would contribute modern DIC, and both plot near the CRET, indicating Colorado River water that has not mixed with detectable amounts of water of other sources. Such mixing would invalidate the application of the Fontes–Garnier method. Using a $\delta^{13}\text{C}_{\text{CaCO}_3}$ value of -5.6‰ (from bulk sediment at site 20), $\delta^{13}\text{C}_{\text{soil-CO}_2}$ value of -23‰ (assumed), partial pressure of CO_2 of 10^{-2} , and a pre-bomb $^{14}\text{C}_0$ of 84 pMC [51] the model yielded corrected ages of 6400 and 18,400 ^{14}C years for sites 13 and 20, respectively. Groundwaters with $\delta^{18}\text{O}$ and $\delta^2\text{H}$ values and low ^{14}C similar to what is observed today at the pozos were not found around the hypothesized recharge zone near Yuma. This suggests that this older water might have been flushed out of the system along the present-day river channel by more contemporary, less-evaporated Colorado River water.

5. Conclusions

A comparison of local recharge, near El Pinacate, with long-term isotope data for rainfall indicates that winter recharge is dominant. Stable and radioactive isotope data suggest that locally derived recharge is not the main source of water supporting the pozos, as suggested by previous studies. Instead, evaporated water derived from the Colorado River is a major component of the pozos recharge. Recharge near the axis of the Colorado River channel occurs with minor evaporation, but in prehistorical times, recharge also occurred at the floodplain margins after being exposed to highly evaporative conditions. Wetland environments where standing water would persist due to the presence of fine-grained material are likely to have played a significant role in the aquifer recharge and are likely to have experienced considerable evaporation.

After infiltration and percolation, groundwater flow direction was influenced by the major faults in the study area. The aquifer underlying the pozos was supplied by evaporated Colorado River water and followed preferential flow paths determined by the local faults. The presence of low permeability material along the fault obstructs flow across the fault, leading to the development of a strongly anisotropic system near the Altar Fault zone that favors groundwater flow parallel to the fault. Groundwater flow direction was likely enhanced by the strong hydraulic gradient generated at the recharge zone.

The Adair pozos are located at the freshwater and seawater interface near the coast. Here, fresh groundwater appeared to be mixing with seawater prior to reaching the surface as suggested by stable isotope and water chemistry data. Tidal surges created during rare, but often occurring, hurricanes likely intensify mixing by forcing seawater above the usual high-tide levels.

The pozos of the Gran Desierto have remained resilient over the centuries despite major landscape changes and water over use in the Colorado River delta. The aquifer feeding the pozos was recharged by evaporated pre-dam Colorado River water. Flow from the river to the pozos occurred at least prior to the 1960s, but perhaps thousands of years ago as suggested by the ^{14}C data. The environment where

recharge occurred is no longer present and the pozos are vulnerable to major groundwater pumping and development in the area.

Supplementary Materials: The following are available online at <http://www.mdpi.com/2076-3263/9/9/378/s1>, Table S1: Ion chemistry and stable isotope data of surface and groundwaters, Table S2: Stable isotopes in rainfall collected at OPCNM.

Author Contributions: Conceptualization, H.A.Z., C.J.E., and B.T.W.; methodology, H.A.Z., C.J.E., and J.C.M.; validation, H.A.Z., C.J.E., and J.C.M.; formal analysis, H.A.Z., C.J.E., J.C.M.; investigation, H.A.Z.; resources, K.W.F., B.T.W., and J.W.; writing—original draft preparation, H.A.Z.; writing—review and editing, C.J.E., K.W.F., B.T.W., J.C.M., J.W.; visualization, H.A.Z. and C.J.E.; supervision, K.W.F., J.C.M.; project administration, H.A.Z., B.T.W., and K.W.F.; funding acquisition, B.T.W., and K.W.F.

Funding: This research was funded in part by the National Park Service Southwest Border Resource Protection Program (SBRPP, Grant No. P16AC00045), and by the University of Arizona ChevronTexaco Geology Summer Fellowship.

Acknowledgments: The authors express their gratitude to the staff at El Pinacate and Gran Desierto de Altar Biosphere Reserve, Organ Pipe Cactus National Monument, and Ejido Vicente Guerrero for their logistics support and assistance during fieldwork.

Conflicts of Interest: The authors declare no conflict of interest.

References

1. Sykes, G. *The Colorado Delta*; Carnegie Institution: Washington, DC, USA, 1937; p. 193.
2. Leopold, A. The Green Lagoons. In *A Sand County Almanac*; Oxford University Press: New York, NY, USA, 1949; pp. 150–158.
3. Ezcurra, E.; Felger, R.; Russell, A.; Equihua, M. Freshwater islands in a desert sand sea: the hydrology, flora, and phytogeography of the Gran Desierto oases of northwestern Mexico. *Desert Plants* **1988**, *9*, 35–44.
4. Glenn, E.P.; Nagler, P.L.; Brusca, R.C.; Hinojosa-Huerta, O. Coastal wetlands of the northern Gulf of California: Inventory and conservation status. *Aquat. Conserv. Mar. Freshw. Ecosyst.* **2006**, *16*, 5–28. [[CrossRef](#)]
5. Felger, R. *Flora of the Gran Desierto and Rio Colorado of Northwestern Mexico*; University of Arizona Press: Tucson, AZ, USA, 2000; p. 673.
6. Felger, R.; Broyles, B. Dry Borders. In *Great Natural Reserves of the Sonoran Desert*; University of Utah Press: Salt Lake City, UT, USA, 2006; p. 816.
7. Glenn, E.P.; Lee, C.; Felger, R.; Zengel, S. Effects of water management on the wetlands of the Colorado River Delta, Mexico. *Conserv. Biol.* **1996**, *10*, 1175–1186. [[CrossRef](#)]
8. Lumholtz, K. *New Trails in Mexico: An Account of One Year's Exploration in North-western Sonora, Mexico, and South-western Arizona, 1909–1910*; Charles Scribner's Sons: New York, NY, USA, 1912; p. 411.
9. Underhill, R.; Bahr, D.; Lopez, B.; Pancho, J.; Lopez, D. *Rainhouse and Ocean: Speeches for the Papago Year*; University of Arizona Press: Tucson, AZ, USA, 1977; p. 153.
10. Mitchell, D.R.; Huckleberry, G.; Rowell, K.; Dettman, D.L. Coastal Adaptations During the Archaic Period in the Northern Sea of Cortez, Mexico. *J. Isl. Coast. Arch.* **2014**, *10*, 28–51. [[CrossRef](#)]
11. Bowen, T. Julian Hayden and the Adair Bay Shell Site. *Kiva* **1998**, *64*, 137–143. [[CrossRef](#)]
12. Hayden, J. *The Sierra Pinacate*; University of Arizona Press: Tucson, AZ, USA, 1998; p. 96.
13. Seager, R.; Ting, M.; Held, I.; Kushnir, Y.; Lu, J.; Vecchi, G.; Huang, H.P.; Harnik, N.; Leetmaa, A.; Lau, N.C.; et al. Model Projections of an Imminent Transition to a More Arid Climate in Southwestern North America. *Science* **2007**, *316*, 1181–1184. [[CrossRef](#)]
14. Ault, T.; Mankin, J.; Cook, B.S. Relative impacts of mitigation, temperature, and precipitation on 21st-century megadrought risk in the American Southwest. *Sci. Adv.* **2016**, *2*, e1600873. [[CrossRef](#)] [[PubMed](#)]
15. Lancaster, N.; Greeley, R.; Christensen, P.R. Dunes of the Gran Desierto Sand-Sea, Sonora, Mexico. *Earth Surf. Proc. Land.* **1987**, *12*, 277–288. [[CrossRef](#)]
16. Beveridge, C.; Korukek, G.; Ewing, R.C.; Lancaster, N.; Morthekei, P.; Singhvi, A.K.; Mahan, S.A. Development of spatially diverse and complex dune-field patterns: Gran Desierto Dune Field, Sonora, Mexico. *Sedimentology* **2006**, *53*, 1391–1409. [[CrossRef](#)]
17. Conner, C.; National Park Service, Tucson, Arizona, USA. Personal communication, 2017.

18. Pacheco, M.; Martín-Barajas, A.; Elders, W.; Espinosa-Cardena, J.M.; Helenes, J.; Segura, A. Stratigraphy and structure of the Altar basin of NW Sonora: Implications for the history of the Colorado River delta and the Salton trough. *Rev. Mex. Cienc. Geol.* **2006**, *23*, 1–22. [[CrossRef](#)]
19. Merriam, R. San Jacinto fault in the northwestern Sonora, Mexico. *Bull. Geol. Soc. Am.* **1965**, *76*, 1051–1054. [[CrossRef](#)]
20. Curray, J.R.; Moore, D.G. Geologic history of the mouth of the Gulf of California. In *Tectonics and Sedimentation Along the California Margin*; Crouch, J.K., Bachman, S.B., Eds.; Society of Economic Paleontologists and Mineralogists: Los Angeles, CA, USA, 1984; Volume 38, pp. 17–36.
21. Gastil, R.G.; Phillips, R.P.; Allison, E.C. Reconnaissance geology of the state of Baja California. *G.S.A. Memoire* **1975**, *140*, 1–170. [[CrossRef](#)]
22. Olmsted, F.; Loeltz, O.; Irelan, B. Geohydrology of the Yuma Area, Arizona and California, Water Resources of Lower Colorado River-Salton Sea Area. *U.S.G.S. Prof. Pap.* **1973**, *486-H*, 1–273.
23. May, R.H. Resource Reconnaissance of the Gran Desierto. Master's Thesis, University of Arizona, Tucson, AZ, USA, May 1973.
24. Dickinson, J.; Land, M.; Faunt, C.; Leake, S.; Richard, E.; Fleming, J.B.; Pool, D.R. Hydrologic Framework Refinement, Ground-Water Flow and Storage, Water-Chemistry Analyses and Water-Budget Components of the Yuma Area, Southwestern Arizona, and Southeastern California. *U.S.G.S Sci. Inv. Rep.* **2006**, *5135*, 1–88.
25. A.D.E.Q. Arizona Department of Water Resources: Well Registry. Available online: <https://gisweb.azwater.gov/waterresourcedata/wellregistry> (accessed on 15 January 2015).
26. CONAGUA. Comisión Nacional del Agua: Actualización de la disponibilidad media anual de agua en el acuífero Valle de San Luis Río Colorado (2601), Estado de Sonora. Available online: https://www.gob.mx/cms/uploads/attachment/file/104293/DR_2601.pdf (accessed on 18 January 2013).
27. Coplen, T.B. Reporting of stable carbon, hydrogen and oxygen abundances. *Ref. Intercomp. Mater. Stable Isot. Light Elem.* **1995**, *825*, 31–34. [[CrossRef](#)]
28. Gieskes, J.; Rogers, W. Alkalinity determinations in interstitial waters of marine sediments. *J. sediment. Res.* **1973**, *43*, 272–277. [[CrossRef](#)]
29. Parkhurst, D.; Appelo, C. User's guide to PHREEQC (version 2) – A computer program for speciation, batch-reaction, one-dimensional transport, and inverse geochemical calculations. *U.S.G.S Water Resour. Inv. Rep.* **1999**, *99*, 1–312.
30. U.S.G.S. Water-Quality Data for the Nation. Available online: <https://water.usgs.gov/owq/data.html> (accessed on 12 December 2016).
31. Palomares-Ramírez, R.B. Identificación de los componentes hidrogeoquímicos que contaminan el acuífero del Modulo de Riego I del Valle de San Luis, R.C. Master's Thesis, Universidad Autónoma de Baja California, Mexicali, México, December 2011.
32. Dettman, D.L.; Flessa, K.W.; Roopnarine, P.D.; Schöne, B.R.; Goodwin, D.H. The use of oxygen isotope variation in shells of estuarine mollusks as a quantitative record of seasonal and annual Colorado River discharge. *Geochim. Cosmochim. Acta* **2004**, *68*, 1253–1263. [[CrossRef](#)]
33. Welker, J. ENSO effects on the isotopic ($\delta^{18}\text{O}$, $\delta^2\text{H}$ and d-excess) of precipitation across the US using a high-density, long-term network (USNIP). *Rapid Comm. Mass Spec.* **2012**, *17*, 1655–1660. [[CrossRef](#)]
34. National Atmospheric Deposition Program (NADP). Available online: <http://nadp.slh.wisc.edu/> (accessed on 5 August 2016).
35. Craig, H. Isotopic variations in meteoric waters. *Science* **1961**, *133*, 213–224. [[CrossRef](#)]
36. Eastoe, C.; Towne, D. Regional zonation of groundwater recharge mechanisms in alluvial basins of Arizona: Interpretation of isotope mapping. *J. Geochem. Explor.* **2018**, *194*, 134–145. [[CrossRef](#)]
37. Robertson, F.N. Geochemistry of groundwater in alluvial basins of Arizona and adjacent parts of Nevada, New Mexico, and California. *U.S.G.S. Prof. Pap.* **1991**, *1406-C*, 1–91.
38. Guay, B.; Eastoe, C.; Basset, R.; Long, A. Identifying sources of groundwater in the lower Colorado River valley, USA with $\delta^{18}\text{O}$, $\delta^2\text{H}$, and ^3H : Implications for river water accounting. *Hydrogeol. J.* **2006**, *14*, 146–158. [[CrossRef](#)]
39. Herczeg, A.L.; Edmunds, W.M. Inorganic Ions as Tracers. In *Environmental Tracers in Subsurface Hydrology*; Cook, P.G., Herczeg, A.L., Eds.; Springer: Boston, MA, USA, 2000; pp. 31–77.
40. Towne, D. Ambient groundwater of the Lower Gila Basin: A 2013–2016 baseline study. *A.D.E.Q. Rep.* **2017**, *17-01*, 1–74.

41. Towne, D. Ambient groundwater of the Western Mexican Drainage: A 2016–2017 baseline study. *A.D.E.Q. Rep.* **2018**, *17-02*, 1–52.
42. Jasechko, S.; Taylor, R. Intensive rainfall recharges tropical groundwaters. *Environ. Res. Lett.* **2015**, *10*, 124015. [[CrossRef](#)]
43. Zamora, H.A. Environmental Isotope Geochemistry in Groundwaters of Southwestern Arizona, USA, and Northwestern Sonora, Mexico: Implications of Groundwater Recharge, Flow, and Residence Time in Transboundary Aquifers. Ph.D. Thesis, University of Arizona, Tucson, AZ, USA, November 2018.
44. Clark, I.; Fritz, P. *Environmental Isotopes in Hydrogeology*; Lewis Publishers: Boca Raton, FL, USA, 1997; pp. 87–88.
45. Braitsch, O. *Salt Deposits, their Origin and Composition*; Springer: New York, NY, USA, 1971; pp. 1–26.
46. Davis, S.N.; Whittemore, D.G.; Fabryka-Marin, J. Uses of chloride/bromide ratios in studies of potable water. *Ground Water* **1998**, *36*, 338–350. [[CrossRef](#)]
47. Gribble, G. The diversity of naturally occurring organobromine compounds. *Chem. Soc. Rev.* **1999**, *28*, 335–346. [[CrossRef](#)]
48. Bense, V.F.; Gleeson, T.; Loveless, S.E.; Bour, O.; Scibek, J. Fault zone hydrogeology. *Earth Sci. Rev.* **2013**, *127*, 171–192. [[CrossRef](#)]
49. Payne, B.; Quijano, L.; Latorre, C. Environmental isotopes in a study of the origin of salinity of groundwater in the Mexicali Valley. *J. Hydrol.* **1979**, *41*, 201–2015. [[CrossRef](#)]
50. Fontes, J.C.; Garnier, J.M. Determination of the initial ¹⁴C activity of total dissolved carbon: A review of existing models and a new approach. *Water Resour. Res.* **1979**, *15*, 325–329. [[CrossRef](#)]
51. Goodfriend, G.; Flessa, K. Radiocarbon Reservoir Ages in the Gulf of California: Roles of Upwelling and Flow from the Colorado River. *Radiocarbon* **1997**, *2*, 139–148. [[CrossRef](#)]



© 2019 by the authors. Licensee MDPI, Basel, Switzerland. This article is an open access article distributed under the terms and conditions of the Creative Commons Attribution (CC BY) license (<http://creativecommons.org/licenses/by/4.0/>).